Electronic Supplementary Material (ESI) for Soft Matter.

Supplementary Information for manuscript "Auxeticity enhancement due to size polydispersity in fcc crystals of hard-core repulsive Yukawa particles"

P. M. Pigłowski, J. W. Narojczyk, K. W. Wojciechowski, and K. V. Tretiakov*

Institute of Molecular Physics, Polish Academy of Sciences,

M. Smoluchowskiego 17, 60-179 Poznań, Poland

E-mail: tretiakov@ifmpan.poznan.pl

Elastic constants and Poisson's ratio

The strain tensor in Parrinello and Rahman method[1] is defined as

$$\epsilon \equiv \frac{1}{2}\left(\mathbf{H}^{-1}\mathbf{hhH}^{-1} - \mathbf{I}\right) \ , \tag{1}$$

where $\mathbf{h}$ is the box matrix tensor, $\mathbf{H}$ is the reference box matrix under pressure p^* and $\mathbf{I}$ is the unit matrix. Elements of the elastic compliance tensor are defined as follows:[2]

$$S_{ijkl} = \beta V_p \left\langle \Delta\varepsilon_{ij} \Delta\varepsilon_{kl} \right\rangle \ , \tag{2}$$

where V_p is the average volume at the pressure p, $\Delta\varepsilon_{ij} = \varepsilon_{ij} - \langle \varepsilon_{ij} \rangle$ and $\langle ... \rangle$ denotes the thermodynamic averaging in the NpT ensemble.

As it has been mentioned in main text, it is convenient to use matrix notation in Voigt's form[3] and the regular symmetry of fcc lattice causes that we have only three independent elastic constants. These elastic constants can be calculated using compliances S11, S12 and S44 in following way:

$$C_{11} = \frac{S_{11} + S_{12}}{(S_{11} - S_{12})(S_{11} + 2S_{12})} + p \ , \tag{3}$$

$$C_{12} = \frac{-S_{12}}{(S_{11} - S_{12})(S_{11} + 2S_{12})} - p \ , \tag{4}$$

$$C_{44} = \frac{1}{S_{44}} + p \ . \tag{5}$$

The Poisson's ratio in the main crystallographic directions for regular symmetry of crystal can be expressed as a function of the elastic constants (C_{ij}):[4]

$$\begin{aligned}
\nu_{[100]} &= \frac{C_{12}+p}{C_{11}+C_{12}}\ , && (6)\\
\nu_{[111]} &= \frac{C_{11}+2C_{12}-2C_{44}+3p}{2(C_{11}+2C_{12}+C_{44})}\ , && (7)\\
\nu_{[110][001]} &= -\frac{4(C_{12}+p)(-C_{44}+p)}{C_{11}^2-2C_{12}^2+C_{11}(C_{12}+2C_{44}-3p)-5C_{12}p-2C_{44}p}\ , && (8)\\
\nu_{[110][1\bar{1}0]} &= \frac{C_{11}^2-2C_{12}^2-5C_{12}p+2(C_{44}-2p)p+C_{11}(C_{12}-2C_{44}+p)}{C_{11}^2-2C_{12}^2+C_{11}(C_{12}+2C_{44}-3p)-5C_{12}p-2C_{44}p}\ . && (9)
\end{aligned}$$

Versor $\hat{\mathbf{n}}$

The versor $\hat{\mathbf{n}}$ is determined by spherical coordinates θ, ϕ as it shown in the figure 1. In the main text, $n(\theta, \phi)$ represents the direction of applied stress, whereas $m(\alpha)$ describes the direction of measurement of Poisson's ratio.

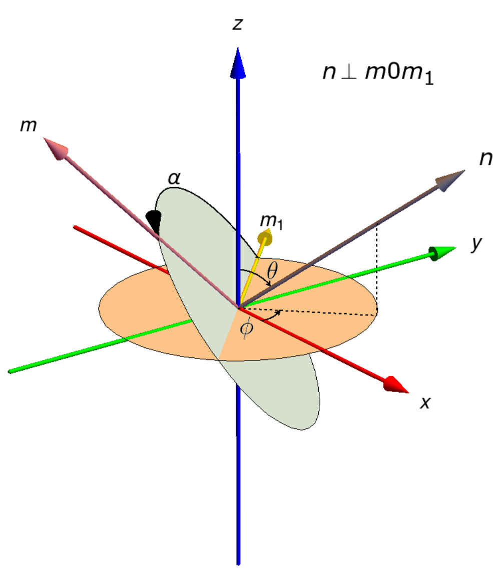

Figure 1: Representation of $\hat{\mathbf{n}}$ and $\hat{\mathbf{m}}$ in spherical coordinates. $m(\alpha)$ is lying in the plane perpendicular to $\hat{\mathbf{n}}$. The angle α is to be measured counterclockwise starting from the direction $\hat{\mathbf{m}}_{\mathbf{1}}$ lying in the plane OXY.

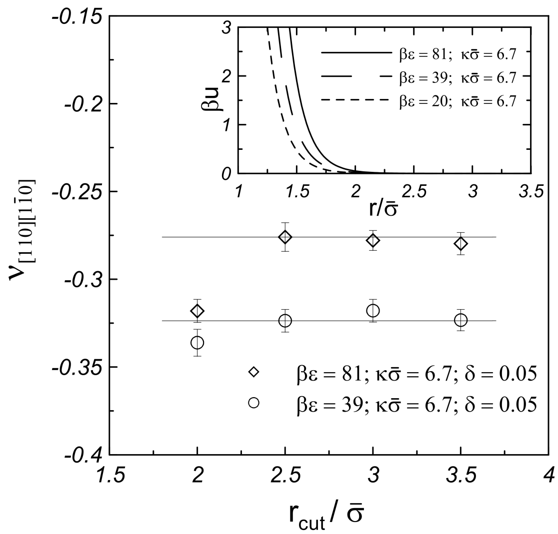

Figure 2: Poisson's ratio in the auxetic direction ($[110][1\bar{1}0]$) versus r_{cut}. By horizontal lines are marked the results obtained for $r_{cut} = 2.5\bar{\sigma}$. The insert represents the pair potentials for two reference particles with $\bar{\sigma}$ for three Yukawa potentials with the longest screening length considered in this study.

Simulation details

Each simulation run was started from a perfect fcc structure, in which diameters of hard-core was taken from Gaussian distribution with a given polydispersity, δ. Simulations for each studied phase point were performed for at least 10 different, independent structures fulfilling the conditions described in Ref.[5] After that the elastic compliances were calculated by averaging over all different structures. More details of preparation of polydisperse sample can be found in Ref.[5] The typical length of simulation run took 6×10^6 MC cycles, of which the first 10^6 cycles were devoted to equilibration of the system.

The following reduced quantities have been used in this paper: the density $\rho = \rho^* \bar{\sigma}^{-3}$, the pressure $p = p^* \frac{k_B T}{\bar{\sigma}^3}$, potential energy $E = E^* k_B T$, elastic moduli $C_{ij} = C^*_{ij} \frac{k_B T}{\bar{\sigma}^3}$, elastic compliance $S_{ij} = S^*_{ij} \frac{\bar{\sigma}^3}{k_B T}$ where by the star ('$*$') denoted dimensionless quantities. The interaction between the particles was truncated at $r_{cut} = 2.5\bar{\sigma}$ and long-range corrections to

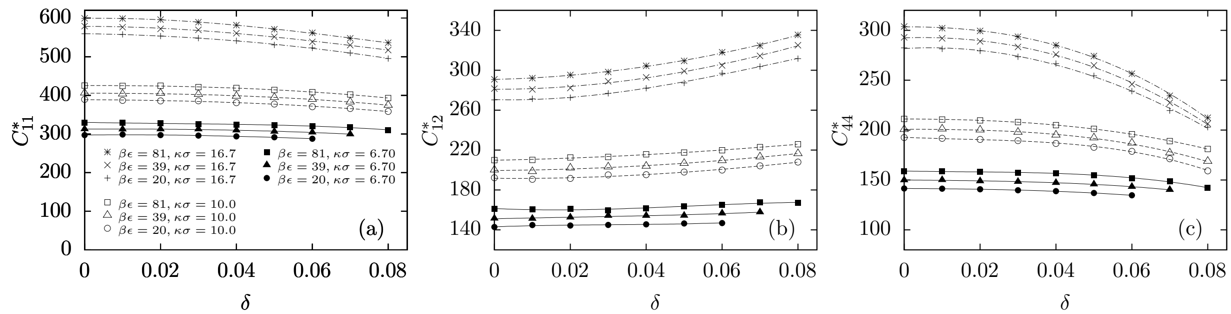

Figure 3: Elastic constants C^*_{ij} ploted with respect to polydispersity parameter for studied values of scrrning lenght and contact potential.

the energy have been taken into account. The choice of such $r_{cut} = 2.5\bar{\sigma}$ follows from the fact that the inter-particle interaction potentials discussed in this paper are of short-range, see the insert in Fig. 2. This choice is quantitatively confirmed by the dependencies of the Poisson's ratio on r_{cut} in the auxetic direction which are shown in Fig. 2. One can see there that in both cases with the longest screening length, the results obtained for $r_{cut} = 2.5\bar{\sigma}$ are in very good agreement with those obtained for longer r_{cut}.

Elastic constants vs particle size polydispersity

The effect of polydispersity on elastic properties can be observed in the dependencies of $C^*_{ij}(\delta)$ for different parameters of Yukawa potential (see Fig. 3). Most essential changes can be seen for the elastic constant C^*_{44} at the shortest screening lengths. From the equations (6)–(9) it is following these changes are reflected directly in the values of the Poisson's ratio (Fig. 4). In the figure one can observe an increase of Poisson's ratio in the directions of [100], [111], and [110][001] with increasing of the polydispersity parameter δ.

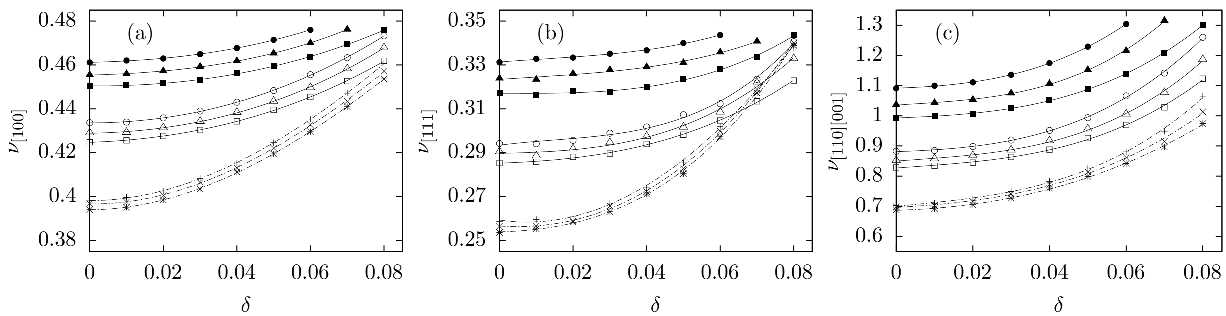

Figure 4: Poisson's ratios $\nu_{[100]}$ (a), $\nu_{[111]}$ (b), $\nu_{[110][001]}$ (c) as a function of polydispersity for $p^* = 60$ and different values of Yukawa parameteres. The legend is the same as in Fig. 3a.

Influence of temperature on auxeticity

All obtained results in this study are given in terms of so-called Yukawa parameters. Another representation of any Yukawa phase point is the $(\lambda,\ \tilde{T})$,[6,7] where $\tilde{T}$ is the dimensionless temperature which is given by[7]

$$\tilde{T} = \left[\frac{2}{3}\lambda^2 \beta u_M(\lambda)\right]^{-1} , \tag{10}$$

and u_M is the Madelung energy per particle in an ideal fcc crystal. $\lambda = \kappa\bar{\sigma}(6\eta/\pi)^{-1/3}$ is a scaled Debye length where η is the packing fraction. Using this representation one can calculate the dependencies of Poisson's ratio in the auxetic direction (for various polydispersity parameters) on temperature which are shown in Fig. 5. One can observe that an increase of temperature enhances auxeticity of the system.

Auxeticity of the system

Let us consider an *ideal* auxetic for which $\nu_{ideal} = -1$ and try to visualize it in a three-dimensional plot. We assume that a vector from the origin of the coordinate system points to some point. A direction of the vector represents the direction of the applied stress $(\hat{\mathbf{n}})$,

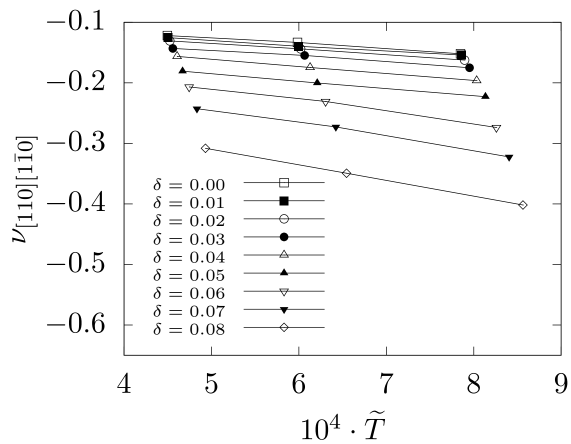

Figure 5: Temperature dependencies of Poisson's ratio in the $[110][1\bar{1}0]$-direction at $p^* = 60$ and $\kappa\bar{\sigma} = 10$ for different values of polydispersity parameter.

and its modulus has the value of the average auxeticity in that direction (average value of the integral of the auxetic area, see Fig. 6a). Thus, the ideal auxetic will be described by a sphere of radius $r_{ideal} = |\nu_{ideal}| = |-1| = 1$ and volume $A_{ideal} = 4\pi/3$, which we will call *ideal auxeticity*(see Fig. 6b). In the case of the studied auxetic, the application of the procedure described above will lead to a complicated geometric shape (Fig. 6d) with a volume of A, which can be referred to volume of a sphere of radius r_s (Fig. 6e). Then, the ratio of the radius of these spheres will determine the *degree of auxeticity* of the given system, namely:

$$\chi = \frac{r_s}{r_{ideal}} = \frac{\sqrt[3]{3A/4\pi}}{\sqrt[3]{3A_{ideal}/4\pi}} = \sqrt[3]{\frac{3A}{4\pi}} \ , \tag{11}$$

where

$$A = \int\limits_0^{2\pi} d\phi \int\limits_0^{\pi} \sin\theta d\theta \int\limits_0^{R(\theta,\phi)} r^2 \mathrm{d}r \ , \tag{12}$$

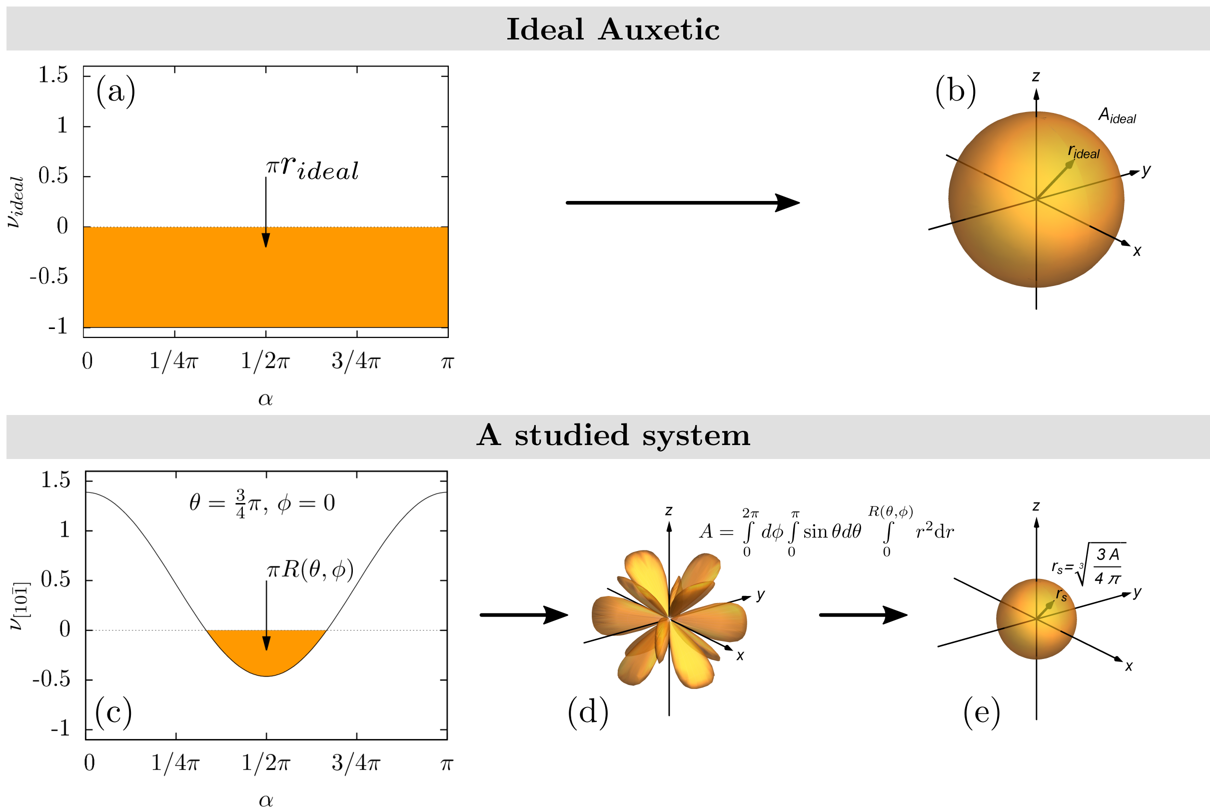

Figure 6: (a) An average negative Poisson's ratio of ideal auxetic. (b) 3D representation of the auxetic properties of the ideal auxetic. (c) The Poisson's ratio with respect to the direction of measurement (designated by α). The shaded area is the measure of the average negative Poisson's ratio of the studied system (Eq. (13)), (d) Representation of the auxetic properties of the studied system in spherical coordinates. The surface consists of the points which created by $R(\theta, \phi)$. θ, ϕ define the direction of $\hat{\mathbf{n}}$. $R(\theta, \phi)$ corresponds to the mean value of Poisson's ratio $\nu_{\hat{\mathbf{n}}}(\alpha)$ in the direction of applied stress ($\hat{\mathbf{n}}$). (e) A sphere of volume of A equal to volume of geometric shape shown in Fig. (d).

and the average over negative values of Poisson's ratio (Fig. 6c) in the direction of $\hat{\mathbf{n}}$ is

$$R(\theta,\phi) = \frac{1}{2\pi}\int\limits_0^\pi \left(\left|\nu_{n(\theta,\phi)}(\alpha)\right| - \nu_{n(\theta,\phi)}(\alpha)\right) \mathrm{d}\alpha \ . \tag{13}$$

References

(1) Parrinello, M.; Rahman, A. Strain fluctuations and elastic constants. *J. Chem. Phys.* **1982**, *76*, 2662–2666.

(2) Wojciechowski, K. W.; Tretiakov, K. V.; Kowalik, M. Elastic properties of dense solid phases of hard cyclic pentamers and heptamers in two dimensions. *Phys. Rev. E* **2003**, *67*, 036121.

(3) Nye, J. F. *Physical Properties of Crystalls, Their Representation by Tensors and Matrices*; Clarendon Press: Oxford, 1957.

(4) Tretiakov, K. V.; Wojciechowski, K. W. Partially auxetic behavior in fcc crystals of hard-core repulsive Yukawa particles. *Phys. Status Solidi B* **2014**, *251*, 383–387.

(5) Tretiakov, K. V.; Wojciechowski, K. W. Elasticity of two-dimensional crystals of polydisperse hard disks near close packing: Surprising behavior of the Poisson's ratio *J. Chem. Phys.*, 2012, **136**, 204506.

(6) Hynninen, A. P.; Dijkstra M. Phase diagrams of hard-core repulsive Yukawa particles *Phys. Rev. E*, 2003, **68**, 021407.

(7) Royall, C. P.; Leunissen M. E.; Hynninen A. P.; Dijkstra M.; van Blaaderen A. Reentrant melting and freezing in a model system of charged colloids *J. Chem. Phys.*, 2006, **124**, 244706.